Tellus (2004), 56A, 47–55
Printed in UK. All rights reserved

TELLUS

Finding the effective parameter perturbations in atmospheric models: the LORENZ63 model as case study

By HANNEKE E. MOOLENAAR[1,2]* and FRANK M. SELTEN,[2] [1]*Group Mathematical and Statistical Methods, Wageningen University, PO Box 100, 6700 AC Wageningen, The Netherlands;* [2]*Royal Netherlands Meteorological Institute (KNMI), PO Box 201, 3730 AE De Bilt, The Netherlands*

(Manuscript received 4 February 2003; in final form 19 September 2003)

ABSTRACT

Climate models contain numerous parameters for which the numeric values are uncertain. In the context of climate simulation and prediction, a relevant question is what range of climate outcomes is possible given the range of parameter uncertainties. Which parameter perturbation changes the climate in some predefined sense the most? In the context of the LORENZ 63 model, a method is developed that identifies effective parameter perturbations based on short integrations. Use is made of the adjoint equations to assess the sensitivity of a short integration to a parameter perturbation. A key feature is the selection of initial conditions.

1. Introduction

Complex numerical models are used to make expectations for the Earth's future climate. The reliability of these expectations is unknown. One contributing factor is the existence of uncertain model parameters which leads to uncertainties in the outcome of the simulations. Ideally one would like to quantify these uncertainties. In IPCC (2001), it is stated that a systematic evaluation of the effect of parameter uncertainties on the simulation of the present climate and the transient climate response is urgently needed. A direct approach, perturbing parameters and making additional climate simulations, is infeasible due to computational constraints. Many expensive simulations are required since the simulated climate is bound to be more sensitive to some parameter changes than to others. It would therefore be of great practical use to be able to identify effective parameter perturbations a priori on the basis of short integrations. However, it is not at all clear that this is possible. Some previous studies shed light on this issue.

Corti and Palmer (1997) presented evidence that sensitivities based on short-term integrations are relevant for changes in long-term statistics. They calculated for a quasi-geostrophic atmospheric model perturbations to initial conditions that maximize the projection of the perturbations after 5 days on to a particular pattern, the NAO or PNA in their case. Next they averaged these optimal perturbations of 2000 initial conditions. This averaged perturbation was put on the right-hand side of the equation as an additional time-invariant forcing. The probability density function (PDF) of the amplitude of the PNA pattern was determined for the reference and the perturbed forcing from a long integration. The result was that the PDF of the PNA pattern changed a lot due to the forcing perturbation and more so than with a forcing perturbation in the direction of the PNA pattern itself. This result suggests that in order to find parameter or forcing perturbations to which the climate is sensitive, use can be made of the sensitivity of short-term evolutions to such perturbations. In our terminology, forcing terms refer to parameters in the tendency equations that are not multiplied by state variables.

Lea et al. (2000) also worked on the idea that short-term evolutions can be used for a sensitivity analysis of the climate. In the LORENZ 63 model (Lorenz, 1963) a brute-force method was used to assess the effect of changes in parameter r on the climate mean. The climate sensitivity was then measured in terms of $\Delta\bar{z}_\infty/\Delta r$, where $\bar{z}_\infty$ is the average value of the variable z over a time interval of length τ, as $\tau \to \infty$. They found that an intermediate time scale τ - exists for which adjoint calculations to determine $\Delta\bar{z}_{\tau*}/\Delta r$, ensemble averaged over a set of initial conditions, gives a reasonable estimate of $\Delta\bar{z}_\infty/\Delta r$. This result is another indication that it makes sense to try to identify effective parameter perturbations on the basis of short-term integrations.

Hall (1986) showed the potency of using the adjoint equations to determine climate sensitivities by determining the sensitivity of the global mean surface air temperature for variation in different model parameters of an atmospheric model with prescribed sea surface temperatures. Using 10-d integrations, the

*Corresponding author.
e-mail: moolenaa@knmi.nl

sensitivities estimated with the use of adjoints agreed to within 20% with the sensitivities obtained directly by rerunning the model. A question remains as to whether this 10-d estimate provides a reasonable estimate for the sensitivity of the temperature averaged over a 30-yr period. Also, it is not clear whether the adjoint equations yield useful sensitivities for longer integrations, since the atmosphere is a chaotic system, for which the evolution depends sensitively on small changes in the initial condition.

In this paper we develop an efficient method that can identify parameter perturbations on the basis of short-term integrations that cause, with high probability, large changes in the simulated climate. In this way, estimates can be obtained of the range of possible climate outcomes given the uncertainties in model parameters. Changes in the probability of certain types of circulation that have a great influence on a regional climate are the main focus. The method is developed in the context of a simple numerical model used as a climate metaphor, namely the LORENZ 63 model, and, motivated by the studies mentioned above, is based on the effect of parameter perturbations on short-term evolutions.

In Section 2 the modified LORENZ 63 model and its characteristics are described. In Section 3 we describe the methods that we used to identify effective parameter perturbations in the LORENZ 63 model. (Effective parameter perturbations are the parameter perturbations that change model simulations the most.) Section 4 contains our conclusions and a discussion.

2. LORENZ63 model

We take the LORENZ 63 model (Lorenz, 1963) as a climate metaphor. It is described by three differential equations, describing the time evolution of state variables x, y and z and contains three parameters, σ', r' and b'. Following Palmer (1999), two additional parameters $c_{x'}$ and $c_{y'}$ are introduced to break the symmetry of the solution:

$$\begin{aligned} \dot{x} &= -\sigma' x + \sigma' y + c'_x, \\ \dot{y} &= -xz + r' x - y + c'_y, \\ \dot{z} &= xy - b' z. \end{aligned} \tag{1}$$

For certain parameter settings, the model solution consists of irregular transitions between two unstable equilibria, which might be thought of, in meteorological terms, as representing blocked or zonal flow regimes. If the parameters in the model are set at their standard values, $(\sigma', r', b', c'_x, c'_y) = (10, 28, \frac{8}{3}, 0, 0) = (\sigma_0, r_0, b_0, c_{x0}, c_{y0})$, the two regimes are equally populated. To characterize their population, we determine from a long simulation the probability density function (PDF) along the vector connecting the two regimes. Prior to this, the time series is low-pass filtered with a running mean of one time unit. The resulting PDF clearly shows the existence of equally populated regimes, see Fig. 1.

A parameter γ, measuring the asymmetry, is introduced. Its value is obtained by integrating the PDF over the left half of its domain, subtract it from 0.5 and multiply by 2. A value of 0 corresponds to a symmetric PDF, which is obtained for the standard values, values of ± 1 are limiting values corresponding to the population of one regime only. Changes in the population of the regimes are of interest, since regime behaviour in climate models has a large influence on regional climates. When compared with blocked or zonal flows, more blocked flows near Europe causes dryer and warmer periods in summer or dryer and colder periods in winter for Western Europe and more wet and stormy weather to the north and south of the blocking (Oortwijn and Barkmeijer, 1995).

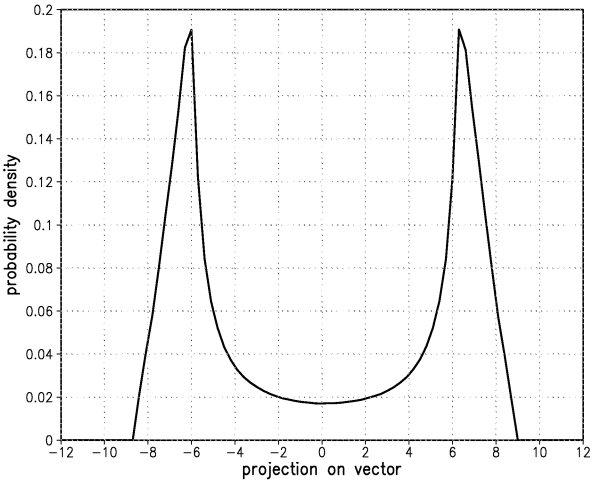

Fig 1. Probability density function of low-pass filtered time series of the projection onto the vector connecting the two regimes, for the LORENZ 63 model with standard parameter values.

We assume that the model parameters are uncertain within $\pm 5\%$ of their standard values ($c_{x'}$ and $c_{y'}$ can vary by ± 1). For mathematical convenience, this is accomplished by choosing a new set of parameters, $(\sigma_0 + 0.5\sigma, r_0 + 1.4r, b_0 + \frac{2}{15}b, c_{x0} + c_x, c_{y0} + c_y)$, where the parameters σ, r, b, c_x, c_y can vary between $[-1, 1]$.

3. Finding the effective parameter perturbations

The question we wish to address is the following: what is the maximum value of γ possible, given the specified uncertainties in the parameters of the LORENZ 63 model. Or, in meteorological terms, does a model allow a climate solution with more blocked flows, leading to more frequent cold spells in winters in Europe for instance. One approach to determine this maximum value of γ, is by the use of the direct method (Dickinson and Gelinas, 1976).

3.1. *The direct method*

The direct method is a 'brute-force' method; random parameter perturbations are drawn from a uniform distribution on a five-dimensional unit-sphere in parameter space, centered around the

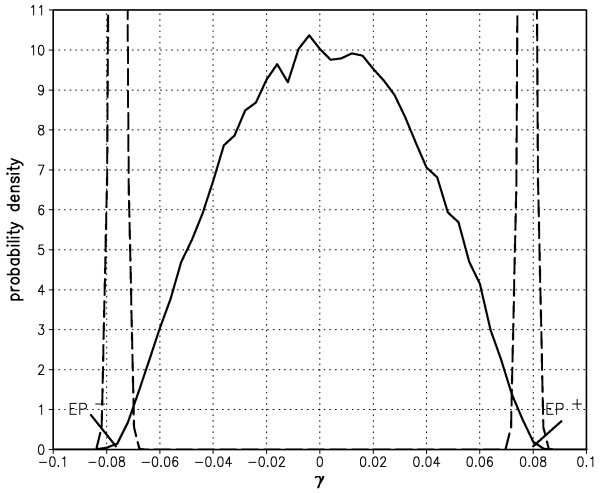

Fig 2. Probability density function of asymmetry γ of randomly chosen parameter perturbations (solid line), together with an idealized PDF (dashed line).

standard values ($(\sigma_0, r_0, b_0, c_{x0}, c_{y0}) = (10, 28, \frac{8}{3}, 0, 0)$). Note that because of the special choice of the parameters, points on this unit-sphere correspond to parameter perturbations that lie within the specified range of 5% uncertainty. For each of these random perturbations, γ is estimated from a long integration (80 000 time units). The length of 80 000 time units allows γ to be estimated to within an absolute error of about 0.001. A total of 50 000 random parameter perturbations were evaluated. The values of γ obtained are displayed in the form of an estimate of the probability density function of γ in Fig. 2 (solid line). The PDF estimate was obtained by dividing the range of γ, $[-0.10, 0.10]$ into 100 bins, counting the number of occurences in each bin and finally dividing by the total number of draws.

The PDF of γ is centered around zero, is uni-modal and is bounded from below by -0.08 and above by 0.08. The maximum is found at zero, which means that the most probable climate solution, given the uncertainties in the parameters, has equal probabilities for both regimes. However, climate solutions are possible with 8% more occurences of one regime. The PDF indicates that the chance of picking a parameter perturbation that leads to such an asymmetric solution is small. Most parameter perturbations lead to fairly symmetric solutions. This means that many draws are needed to estimate the range of possible values of γ. Therefore it would be of great practical use to be able to draw effective parameter perturbations, that is perturbations that most effectively change γ, a priori, also since long simulations are computationally demanding. Ideally one would like to draw effective parameter perturbations only, as indicated by the idealized PDF in Fig. 2 (dashed line). We wish to determine these on the basis of short model simulations. That this might be possible is based on the notion that systematic changes in short-term evolutions change long-term statistics.

3.2. *The adjoint method*

3.2.1. Effective parameter perturbations and short-term integrations. To follow up on this idea, we choose two sets of effective parameter perturbations from the tails of the distribution of γ in Fig. 2, which we call EP^+ and EP^-, and investigate the effect of these perturbations on short model evolutions in order to find a means to detect these effective parameter perturbations a priori on the basis of short model evolutions alone. Our short integrations take 2 time units. This is sufficiently long for a regime transition to take place as well as sufficiently short for the linear approximation to still be accurate enough in most cases. For a realistic atmospheric model, this range would be 3–5 d (Oortwijn and Barkmeijer, 1995).

In Fig. 3 two short-term evolutions of 2 time units, for unperturbed parameters, referred to as a reference orbit are plotted. In Figs. 3a and c we also plotted the end points of additional evolutions from the same initial condition but with randomly perturbed parameters (grey and black points). In Figs. 3b and c the end points of orbits with the selected perturbed parameters EP^+ (black) and EP^- (grey) are plotted. The two regimes are indicated by the large grey and black dot. The black points in Figs. 3a and c are calculated using the non-linear equations (1), whereas the grey points in Figs. 3a and c, and EP^+ and EP^- in 3(b) and (d) are calculated using a linear approximation of the equations around the reference orbit, referred to as the tangent linear equations.

Using the tangent linear equations, a cheap method exists to calculate the parameter perturbation yielding the largest deviation at the end of the reference orbit. The method is based on a singular-value decomposition (SVD) of the linear mapping of the parameter perturbation on to the changes in the end point of the reference orbit. The first right singular vector corresponds to the parameter perturbation and is mapped on to the first left singular vector, which corresponds to the direction of largest change of the end point of the reference orbit. The corresponding singular value equals the length of the left singular vector. The method is described in the appendix and is very similar to the procedure for finding the perturbation to the initial conditions yielding the largest change at the end of the reference orbit (Barkmeijer, 1996).

The linearly evolved random parameter perturbations (grey points) in Figs. 3a and c form an ellipsoid centered around the end point of the reference orbit (black line). The deviation of the black cloud from the grey one is an indication of the limited accuracy of the linearized solution. This accuracy depends on the magnitude of the deviations from the reference orbit (δ **g**, see the appendix) which grow in time, for some reference orbits faster than for others.

Focussing on the effective perturbations EP^+ and EP^-, we observed that for some reference orbits they do not lie in distinct areas of the cloud (Fig. 3b), but that for others EP^+ and EP^- are clearly separated and lie on the end points of the first left singular

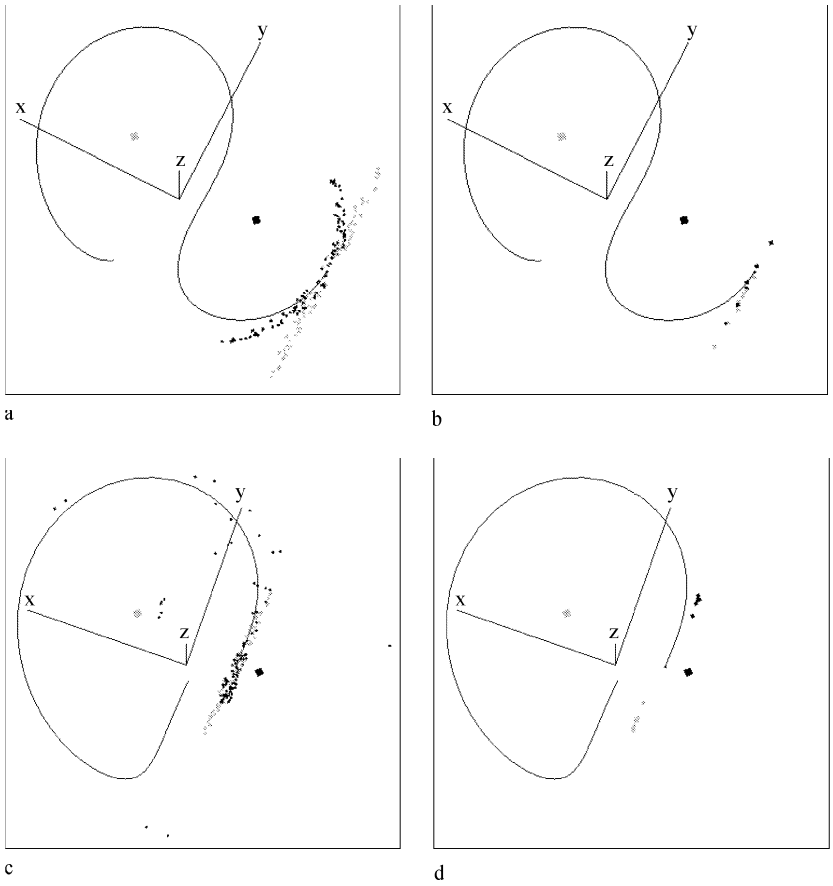

Fig 3. The black line is a reference orbit of 2 time units in the 3-D state space of the LORENZ 63 model. The two regimes are indicated by the large grey and black dot. In (a) and (c) the grey and black points are respectively the linearly and non-linearly evolved random parameter perturbations, all from the same initial condition. In (b) and (d) the grey and black points are EP^- and EP^+, respectively. In (b) EP^- and EP^+ do not lie in distinct area's. In (d) EP^- and EP^+ are clearly separated and lie on the ends of the first left singular vector. Note also that the change induced by the parameter perturbations is not directed along the vector connecting both regimes, but instead is almost perpendicular to it.

vector, as shown in Fig. 3d. Thus for reference orbits like this one, the first right singular vector is likely to be an effective parameter perturbation.

The only problem is how to select orbits such as in Fig. 3d without any knowledge of EP^+ and EP^-. By shifting reference orbits in time one timestep after another and examining the behaviour of EP^+ and EP^-, we discovered that the separation along the first singular vector takes place just after an episode when the first singular value has grown to very large values. As an illustration of this, we have plotted the first singular value for subsequent reference orbits in time in Fig. 4. Every now and then the singular value exceeds 8000 and comes down again below 220. At this moment, EP^+ and EP^- are separated along the first left singular vector, and the first right singular vector is likely to be an effective parameter perturbation. This empirical finding gives us a recipe to draw potentially effective parameter perturbations a priori:

(1) shift the reference orbit in time;

(2) select a reference orbit according to the evolution of the first singular value (after a period of extensive growth);

(3) determine for that reference orbit the first singular vector using the adjoint method, use this as a parameter perturbation.

For the computation of the first singular vector and the value corresponding to a reference orbit, one needs to calculate this reference orbit (this is a non-linear integration of 2 time units), the tangent linear and the adjoint equations (both at the cost of twice that of a non-linear integration of 2 time units). This is a total cost of five times a non-linear integration of 2 time units. In Fig. 4 it is shown that on average the first singular value exceeds 8000 four times per 200 shifts of the reference orbit in time. So on average one needs to shift the reference orbit in time 50 times before finding a suitable initial condition. So the total cost to find an effective parameter perturbation is $50 \times 5 \times 2 = 500$ time units of a non-linear integration, which is only a fraction of the 80 000 time units needed for one long-term non-linear climate integration. Since this method of finding

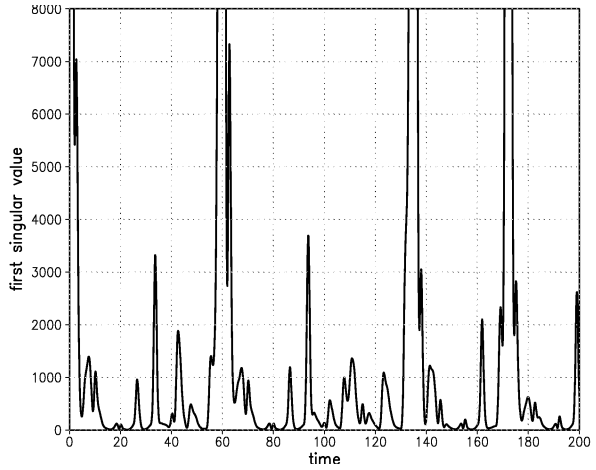

Fig 4. A plot of the first singular value which measures the maximum change possible in the end state of the reference orbit. The reference orbit has a duration of 2 time units and is shifted in time in discrete steps of 0.1 time unit.

effective parameter perturbations has so little computational cost compared with one long-term non-linear integration, it is relevant to use this method to select effective parameter perturbations a priori instead of perturbing at random and making a long-term integration for each of these perturbations.

3.2.2. Effectiveness of the adjoint method. To evaluate the effectiveness of the parameter perturbations determined from the first singular value of selected initial conditions as described above, we made long integrations of 80 000 time units for a total of 50 000 parameter perturbations and calculated γ for each one of these, as we did with the direct method. The PDF of γ is shown in Fig. 5a.

The solid line is the PDF of γ of randomly chosen parameter perturbations, the dashed line is the PDF of γ of the potentially effective parameter perturbations. It is quite clear that the adjoint method applied to specially selected initial conditions draws almost no parameter perturbation that leads to a symmetrical PDF of the LORENZ 63 model ($\gamma = 0$) and has a much higher probability to draw effective parameter perturbations than the random method does. In Fig. 5b the cumulative distribution of both the direct (solid line) and adjoint (dashed line) method are shown. This is the probability to draw a parameter perturbation that yields $|\gamma| \geq x$. For example, the probability to draw parameter perturbations that gives an asymmetry higher than 6%, that is $|\gamma| \geq 0.06$ with the direct method is 7.7%, whereas with the adjoint method this probability is 17.8%, which is 2.29 times as high. This result is proof that sensitivities based on short integrations contain valuable information on the sensitivity of long-term statistics to parameter perturbations, at least for the LORENZ 63 model.

Inspecting the PDF of the adjoint method in Fig. 5a again, it seems that there are two groups of parameter perturbations, one more effective than the other. These perturbations might be related to two sets of reference orbits from which they were

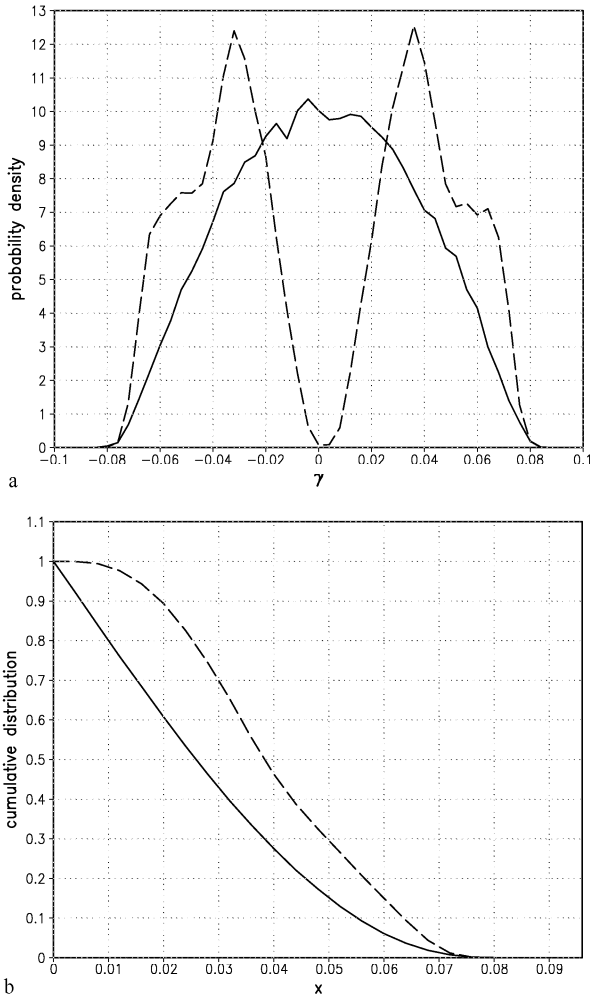

Fig 5. (a) Probability density function of the asymmetry γ. The solid line is the PDF of randomly chosen parameter perturbations, the dashed line is the PDF of parameter perturbations calculated with our adjoint method. (b) Cumulative distribution of both the direct (solid line) and adjoint (dashed line) method. This is the probability to draw a parameter perturbation that yields $|\gamma| \geq x$.

calculated that lie on different areas of the attractor. In Fig. 6 the 25 000 initial values of the reference orbits are plotted that were used to calculate the perturbations (we used both the first singular vector and the opposite signed first singular vector as parameter perturbations to obtain 50 000 draws).

We can divide the initial values broadly into two sets. Set 1 contains the initial conditions in the centre part, set 2 contains the two groups of initial values at the left- and right-hand sides of the attractor. We made separate PDFs of γ of these two sets (see Fig. 7). The dashed line is the same PDF as in Fig. 5a, for all the initial conditions, the dotted dashed line is the PDF for set 1 and the dotted line for set 2. The reference orbits with initial values from set 1 yield more effective parameter perturbations

Fig 6. Initial conditions of the reference orbits just after an episode when the first singular value has grown to very large values.

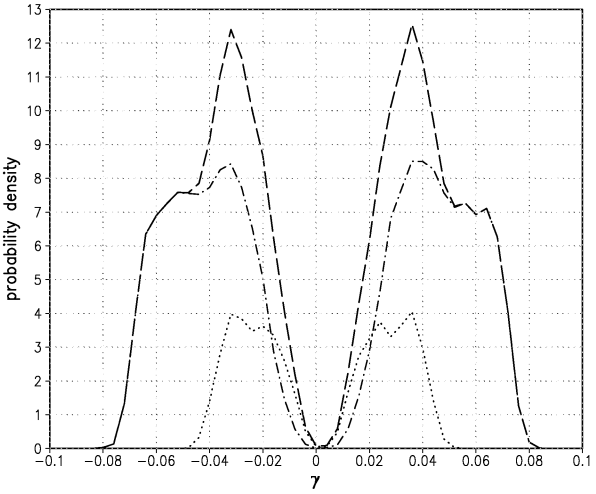

Fig 7. Probability density function of the asymmetry γ. The dashed line is the PDF of parameter perturbations of the adjoint method (as in Fig. 5a), for all initial conditions shown in Fig. 6. The dotted dashed line is the PDF for the set of initial conditions in the centre part in Fig. 6 (set 1) and the dotted line is the PDF for the set of initial conditions on the left- and right-hand sides of the attractor in Fig. 6 (set 2).

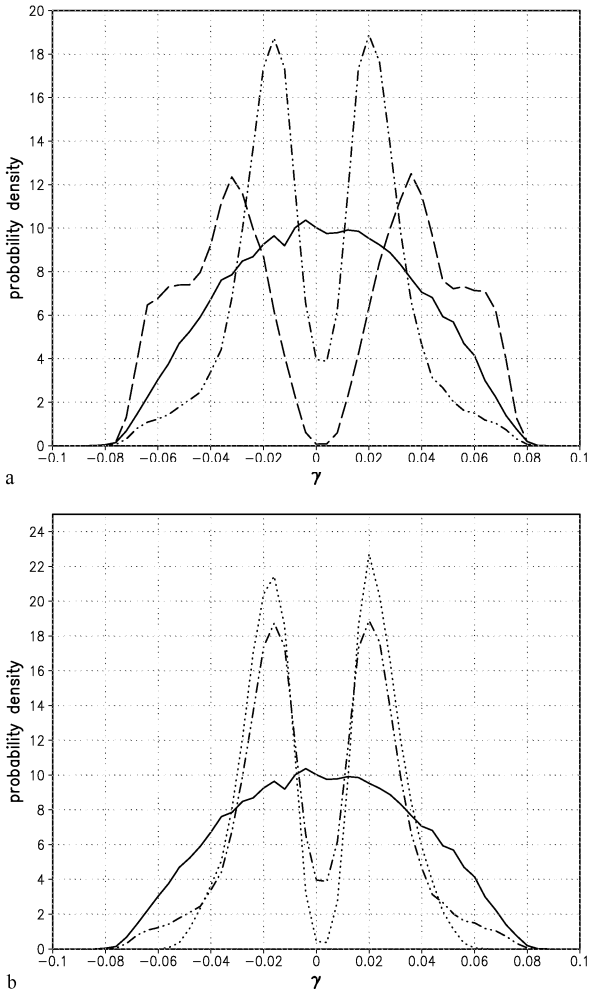

Fig 8. Probability density functions of the asymmetry γ. The solid line in (a) and (b) is the PDF for the direct method (as in Figs. 2 and 5a). In (a) and (b) the dotted dashed line is the PDF of γ taking as parameter perturbations the first singular vector of arbitrary initial conditions. The dotted PDF in (b) is the PDF where parameter perturbations correspond to first singular vectors with very large corresponding singular values only.

than set 2. Unfortunately, this is an observation after the fact and cannot be used to make the adjoint method more effective.

We performed an extra experiment to make sure that the initial conditions, selected after the reference orbit passed through a sensitive area on the attractor, yield effective parameter perturbations. For this, we took the first singular vector as a parameter perturbation for reference orbits 0.1 time unit apart irrespective of the value of the first singular value. For 50 000 perturbations γ was calculated on the basis of 80 000 time unit long trajectories. This gave us the PDF of γ shown in Fig. 8a with a dotted dashed line. Clearly this method is not optimal for drawing effective parameter perturbations. Although this method still gives fewer ineffective parameter perturbations than the random method, it also gives less effective ones. Furthermore, the peaks of the PDF correspond to smaller values of γ than the two highest peaks of the dashed PDF based on the selection of specific initial conditions.

In another experiment to verify the effectiveness of our adjoint method, we took only first left singular vectors as our parameter perturbations, with very large corresponding singular values (greater than 8000). Again, for 50 000 perturbations γ was calculated on the basis of 80 000 time unit long trajectories. This gave us the dotted PDF in Fig. 8b. This is hardly an improvement of the previous PDF in Fig. 8a. Although there are fewer parameter perturbations drawn that give a value γ close to 0, there are

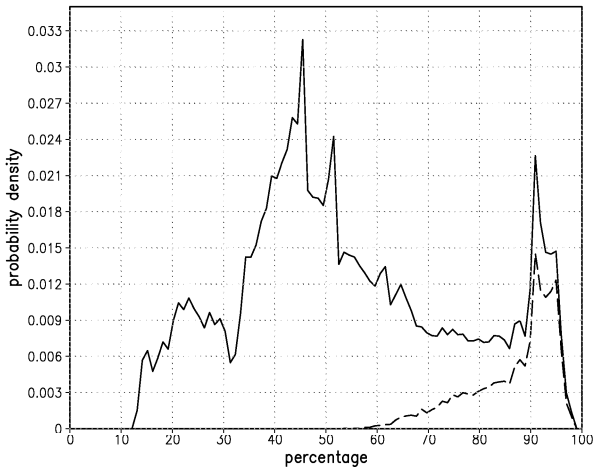

Fig 9. PDF of the percentages of the length of the projection of the singular vector on to the (c_x, c_y)-plane compared with the length of the singular vector, drawn with the adjoint method.

also no parameter perturbations that give a value $|\gamma|$ greater than 0.06.

Another interesting aspect is the contribution of the forcing parameters c_x and c_y to the asymmetry of the model. To illustrate this, we project the first singular vector on to the (c_x, c_y)-plane and calculated the percentage of this length compared with the total length of the first singular vector. We did this for all the singular vectors drawn with the adjoint method, which were used as parameter perturbations. We plotted a PDF of these percentages in Fig. 9. The solid line represents the percentages of all the singular vectors drawn with the adjoint method, the dashed line represents the percentages of the singular vectors that cause an asymmetry higher than 6%. The solid line has two large peaks, one around 45% and one around 92%. The dashed line has one peak around 92%. This does indicate that the forcing parameters c_x and c_y play an important role in causing asymmetry, however, it is also possible to cause a large asymmetry with a contribution of c_x and c_y of for instance 60%, so it is useful to take all parameters into consideration when making perturbations.

To conclude, the adjoint method yields effective parameter perturbations for specific initial conditions that can be selected a priori based on the history of the behaviour of the first singular value.

4. Conclusions and discussion

In this study we set out to develop an efficient method to identify parameter perturbations that cause large changes in the simulated climate. The method is based on the sensitivity of short integrations to parameter perturbations. These sensitivities can be calculated efficiently using the adjoint method (Errico, 1997). The method is developed in the context of the LORENZ 63 equations. It turns out that for specific initial conditions, the parameter perturbations that give rise to the largest changes in the short term also tend to be effective in changing the long-term climate statistics as measured by the asymmetry of the PDF. A priori selection of these special initial conditions is possible. They tend to occur just *after* the trajectory has passed through a very sensitive area where small parameter perturbations can cause the largest changes in the short-term evolution. We do not know why this is, but we do know that parameter perturbations for reference orbits with the largest short-term sensitivities are not effective in perturbing the climate solution.

Since this method of selecting parameter perturbations within the specified uncertainties has a higher probability of drawing effective parameters than the direct method, it is more likely that a good estimate of the largest changes possible in the simulated climate can be obtained with this method when only making a few long-term integrations. One provision must be made; adjoint equations of the model under consideration are needed to determine the short-term sensitivities efficiently. Only a few climate integrations can be made for realistic models due to computational constraints. It pays to identify potentially effective parameter perturbations a priori; probably more so for higher-dimensional systems. It is well known that for atmospheric models most perturbations to initial conditions are rather ineffective since they decay in most of the dimensions in the state space. For similar reasons, most parameter perturbations are bound to be ineffective. There are a relatively low number of unstable directions.

The customary adjoint equations for estimating sensitivities of short-term trajectories to changes in the initial conditions need to be expanded to include the effect of changes in parameters as well. A first step in this direction was taken by Barkmeijer et al. (2002) who included the effect of changes of the forcing terms in the right-hand side of the tendency equations. The most effective changes to the forcing terms for a given reference orbit were called forcing singular vectors.

In this study we have shown the relevance of short-term sensitivities for the sensitivity of long-term statistics for parameter changes. Also Corti and Palmer (1997) presented evidence that sensitivities based on short-term integrations are relevant for long-term statistics. In their study, they ensemble averaged over 2000 initial conditions the perturbation to the initial condition that changed the projection of the end point of a 5-d integration on to the PNA pattern the most and put their averaged perturbation as a forcing perturbation on the right-hand side of the equations. Although they noted a large change in the PDF of the PNA pattern due to this forcing, a question remains as to whether this is the maximum change possible given the size of the forcing perturbation. To answer this question in the context of the LORENZ 63 model, we performed a similar analysis. We determined parameter perturbations that maximize the projection of the end points of the perturbed reference orbit on to the vector connecting both regimes. For a total of 50 000 initial conditions, we determined the mean parameter perturbation. This mean perturbation was scaled to correspond to the specified uncertainty

of 5%. This perturbation yields an asymmetry γ of only 5% of the maximum γ possible, indicating that just averaging optimal perturbations will not necessarily yield an effective parameter perturbation. In contrast, our results indicate that the initial condition of the reference orbit matters.

Lastly, so far the method has only been tested in the context of the LORENZ 63 model. A natural next step is to evaluate the method in the context of a more realistic atmospheric model. Work along these lines is under way.

5. Acknowledgment

We would like to thank J. Grasman for his interest and suggestions.

6. Appendix: the tangent linear equations

Usually, the tangent linear equations are derived for deviations in the state space variables only. Here we include perturbations in model parameters as well. For this purpose, we introduce the vector $\mathbf{q}$, which consists of the vector $\mathbf{x} = (x, y, z)$ in state space and the vector $\boldsymbol{\alpha} = (\sigma, r, b, c_x, c_y)$ in parameter space, so

$$\mathbf{q} = \begin{pmatrix} \mathbf{x} \\ \alpha \end{pmatrix}, \dot{\mathbf{q}} = \begin{pmatrix} \dot{\mathbf{x}} \\ \dot{\alpha} \end{pmatrix} = \begin{pmatrix} \mathbf{F}_1(\mathbf{x}, \alpha) \\ \mathbf{F}_2(\alpha) \end{pmatrix} = \begin{pmatrix} \mathbf{F}_1(\mathbf{x}, \alpha) \\ \mathbf{0} \end{pmatrix} = \mathbf{F}(\mathbf{q}).$$

The tangent linear equations are derived as follows:

$$\begin{aligned} \dot{\mathbf{q}} = \mathbf{F}(\mathbf{q}) &\Rightarrow (\dot{\mathbf{q}_\mathbf{r}} + \dot{\delta\mathbf{q}_\mathbf{r}}) = \mathbf{F}(\mathbf{q}_\mathbf{r} + \delta\mathbf{q}_\mathbf{r}) \\ &\approx \mathbf{F}(\mathbf{q}_\mathbf{r}) + J\delta\mathbf{q}_\mathbf{r} + \mathcal{O}(|\delta\mathbf{q}_\mathbf{r}|^2) \\ &\Rightarrow \dot{\mathbf{q}_\mathbf{r}} + \dot{\delta\mathbf{q}_\mathbf{r}} \approx \mathbf{F}(\mathbf{q}_\mathbf{r}) + J\delta\mathbf{q}_\mathbf{r} \\ &\Rightarrow \dot{\delta\mathbf{q}_\mathbf{r}} \approx J\delta\mathbf{q}_\mathbf{r} \end{aligned}$$

where J is the Jacobi matrix, $\mathbf{q}_\mathbf{r}$ denotes the reference orbit and where

$$\begin{aligned} J &= \left.\frac{\partial \mathbf{F}(\mathbf{q})}{\partial \mathbf{q}}\right|_{\mathbf{q}_\mathbf{r}} = \left.\begin{pmatrix} \dfrac{\partial \mathbf{F}_1(\mathbf{x}, \alpha)}{\partial \mathbf{x}} & \dfrac{\partial \mathbf{F}_1(\mathbf{x}, \alpha)}{\partial \alpha} \\ \dfrac{\partial \mathbf{F}_2(\alpha)}{\partial \mathbf{x}} & \dfrac{\partial \mathbf{F}_2(\alpha)}{\partial \alpha} \end{pmatrix}\right|_{\mathbf{q}_\mathbf{r}} \\ &= \left.\begin{pmatrix} \dfrac{\partial \mathbf{F}_1(\mathbf{x}, \alpha)}{\partial \mathbf{x}} & \dfrac{\partial \mathbf{F}_1(\mathbf{x}, \alpha)}{\partial \alpha} \\ \mathbf{0} & \mathbf{0} \end{pmatrix}\right|_{\mathbf{q}_\mathbf{r}} \end{aligned}$$

the tangent linear equations of the LORENZ 63 model (1) read as

$$\begin{aligned} \dot{\delta x} &= -\sigma' \cdot (\delta x - \delta y) - (x - y) \cdot \delta\sigma' + \delta c'_x, \\ \dot{\delta y} &= (r' - z') \cdot \delta x - \delta y - x \cdot \delta z' + x \cdot \delta r' + \delta c'_y, \\ \dot{\delta z} &= y \cdot \delta x + x \cdot \delta y - b' \cdot \delta z - z \cdot \delta b', \\ \dot{\delta\sigma'} &= 0, \\ \dot{\delta r'} &= 0, \\ \dot{\delta b'} &= 0, \\ \dot{\delta c'_x} &= 0, \\ \dot{\delta c'_y} &= 0. \end{aligned}$$

For a given reference orbit of duration T the tangent linear equations project perturbations in vector $\mathbf{q}$ at the initial time on to perturbations in $\mathbf{q}$ at the final time. Formally, this linear transformation can be represented by a matrix R: $\delta\,\mathbf{q}(T) = R(0, T) \cdot \delta\,\mathbf{q}(0)$, also referred to as the tangent linear propagator. We only wish to assess the influence of parameter perturbations on the flow, not of perturbations in the initial conditions, which means that $\delta\,\mathbf{x}(0) = \mathbf{0}$ and $\delta\,\boldsymbol{\alpha}(0) \neq \mathbf{0}$. To achieve this, projection matrices P_1 and P_2 are introduced that project vector $\mathbf{q}$ into parameter space or state space, respectively:

$$P_1\mathbf{q} = P_1 \begin{pmatrix} \mathbf{x} \\ \alpha \end{pmatrix} = \begin{pmatrix} \mathbf{0} \\ \alpha \end{pmatrix}, \; P_2\mathbf{q} = P_2 \begin{pmatrix} \mathbf{x} \\ \alpha \end{pmatrix} = \begin{pmatrix} \mathbf{x} \\ \mathbf{0} \end{pmatrix}.$$

Using these matrices, a forward integration of the tangent linear equations can be rewritten as

$$P_2 R P_1 \delta\mathbf{q}(0) = \delta\mathbf{x}(T) \equiv S\delta\mathbf{q}(0).$$

When $\delta\,\mathbf{q}(0)$ is limited to a hypersphere, $\delta\,\mathbf{x}(T)$ lies on an ellipsoid. Now, for the length of vector $\delta\,\mathbf{x}(T)$ we can write

$$\begin{aligned} \langle \delta\mathbf{x}(T), \delta\mathbf{x}(T) \rangle^{1/2} &= \langle S\delta\mathbf{q}(0), S\delta\mathbf{q}(0) \rangle^{1/2} \\ &= \langle S^{\mathrm{T}} S\delta\mathbf{q}(0), \delta\mathbf{q}(0) \rangle^{1/2} \end{aligned}$$

where $\langle , \rangle$ defines a euclidean inner product and S^{T} is the transpose of S. This length is maximized when $\delta\,\mathbf{q}(0)$ is the eigenvector of $S^{\mathrm{T}}S$ with the largest eigenvalue. It corresponds to the vector of parameter perturbations that evolves into the major axis of the ellipsoid at time T. The square root of the eigenvalue corresponds to the length of the major axis and is an indication of the sensitivity of the reference orbit to changes in the parameters.

In the literature, this vector is called the first right singular vector, the corresponding eigenvalue the first singular value. This terminology stems from the singular-value decomposition of S (see for instance Press et al. 1986). An arbitrary $(m \times n)$ matrix S can be written as $S = UWV^{\mathrm{T}}$, where U is a column-orthonormal $(m \times n)$ matrix (containing the left singular vectors), W is an $(n \times n)$ diagonal matrix with positive and zero elements (the singular values) and V^{T} is the transpose of the orthonormal $(n \times n)$ matrix V (containing the right singular vectors). These singular vectors are eigenvectors of $S^{\mathrm{T}}S$:

$$\begin{aligned} S^{\mathrm{T}}SV &= (UWV^{\mathrm{T}})^{\mathrm{T}}(UWV^{\mathrm{T}})V \\ &= VWU^{\mathrm{T}}UWV^{\mathrm{T}}V = VW^2V^{\mathrm{T}}V = VW^2 \end{aligned}$$

with eigenvalues equal to the squares of the singular values W. Matrix S projects the right singular vectors on to the left singular vectors:

$$SV = UWV^{\mathrm{T}}V = UW.$$

Thus the left singular vectors are the axes of the ellipsoid.

References

Barkmeijer, J. 1996. Constructing fast-growing perturbations for the nonlinear regime. *J. Atmos. Sci.* **53**, 2838–2851.

Barkmeijer, J., Iversen, T. and Palmer, T. N. 2002. Forcing singular vectors and other sensitive model structures. *Q. J. R. Meteor. Soc.* **12**, 2401–2424.

Corti, S. and Palmer, T. N. 1997. Sensitivity analysis of atmospheric low-frequency variability. *Q. J. R. Meteorol. Soc.* **123**, 2425–2447.

Dickinson, R. P. and Gelinas, R. J. 1976. Sensitivity analysis of ordinary differential equation systems—a direct method. *J. Comp. Phys.* **21**, 123–143.

Errico, R. M. 1997. What is an adjoint model? *Bull. Amer. Soc.* **78**, 2576–2591.

Hall, M. C. G. 1986. Application of adjoint sensitivity theory to an atmospheric general circulation model. *J. Atmos. Sci.* **43**, 2644–2651.

IPCC 2001. Climate Change 2001: The Scientific Basis. Contribution of Working Group I to the Third Assessment Report of the Intergovernmental Panel on Climate Change (eds.J. T. Houghton, Y. Ding, D. J. Griggs, M. Noguer, P. J. van der Linden, X. Dai, K. Maskell and C. A. Johnson). Cambridge University Press, Cambridge, pp. 511

Lea, D. J., Allen, M. R. and Haine, T. W. N. 2000. Sensitivity analysis of the climate of a chaotic system. *Tellus* **52A**, 523–532.

Lorenz, E. N. 1963. Deterministic nonperiodic flow. *J. Atmos. Sci.* **20**, 130–141.

Oortwijn, J. and Barkmeijer, J. 1995. Perturbations that optimally trigger weather regimes. *J. Atmos. Sci.* **52**, 3932–3944.

Palmer, T. N. 1999. A nonlinear dynamical perspective on climate prediction. *J. Climate* **12**, 575–591.

Press, W. H., Flannery, B. P., Teukolsky, S. A. and Vetterling, W. T. 1986. *Numerical Recipes* Section 2.6. Cambridge University Press, Cambridge.